Annular-Ring Slot Antenna Designs with Circular Polarization Radiation

C. Y. D. Sim,[1] W. C. Weng,[2] M. H. Chang,[1] B. Y. Chen[1]

[1]Department of Electrical Engineering, Feng Chia University, Taichung 40724, Taiwan
[2]Department of Electrical Engineering, National Chi Nan University, Puli, 54561, Taiwan

Received 19 August 2014; accepted 12 October 2014

ABSTRACT: The design of a microstrip-fed annular-ring slot antenna (ARSA) with circular polarization (CP) radiation is initially studied. To obtain CP radiation with broad 3-dB axial ratio (AR) bandwidth that can cover the WiMAX 2.3 GHz (2305–2320 MHz, 2345–2360 MHz) and WLAN 2.4 GHz (2400–2480 MHz) bands, a novel technique of extending an inverted L-shaped slot from the bottom section of the annular-ring is proposed. To suppress the harmonic modes induced by the CP ARSA, the technique of integrating a defected ground structure into the annular-ring slot is further introduced. From the measured results, 10-dB impedance bandwidth and 3-dB AR bandwidth of 44.86 and 9.68% were achieved by the proposed harmonic suppressed CP ARSA. Furthermore, average gain and radiation efficiency of ~4.7 dBic and 71%, respectively, were also exhibited across the bands of interest. © 2014 Wiley Periodicals, Inc. Int J RF and Microwave CAE 25:337–345, 2015.

Keywords: annular-ring slot antenna; circular polarization; WLAN; WiMAX; harmonic suppression

I. INTRODUCTION

The main advantages of applying circularly polarized (CP) antenna into the wireless communication system are because of its abilities to mitigate multipath interference and polarization mismatch between the transmitter and receiver. Thus, printed CP antenna on a single layer substrate has been the preferred candidate by the antenna industry, because of the advantages such as low-cost, low profile and ease in manufacturing. However, printed patch antennas usually demonstrate narrow CP bandwidth of $<1\%$ [1], therefore, in order to obtain broad CP bandwidth, much attention has been shifted to the design of printed slot antenna with microstrip-fed or CPW-fed [2–5].

Amid all types of slot antenna designs that have been reported to excite CP radiation, the ring slot antenna designs were studied because of its broad CP bandwidth characteristic [6–8]. To induce good CP radiation, the technique of introducing proper asymmetry in the ring slot and feeding the ring slot using a microstrip line at 45° from the introduced asymmetry was reported [6]. However, this design has demonstrated a slightly narrow CP bandwidth (or 3-dB AR bandwidth) of ~3.5%, and it has a ground plane size of $80 \times 80 \times 1.6$ mm^3. To improve the CP bandwidth to ~8.4%, a simple technique of selecting a proper shorted section in the ring slot was reported [7], however, compared with the design in [6], the size of this reported antenna was very much larger at $140 \times 140 \times 1.6$ mm^3. Therefore, the technique of feeding an annular-ring slot antenna (ARSA) by using a double-bent microstrip-line, and further introducing a vertical slot into the bottom section of the ARSA was investigated [8]. Although this reported design can obtain both compact size ($60 \times 60 \times 1.6$ mm^3) and broad CP bandwidth (9%, 2285–2520 MHz) that can cover both WiMAX 2.3 GHz and WLAN 2.4 GHz applications, however, because of its complicated double-bent microstrip-line fed structure, a number of vital parameters must be tuned concurrently to obtain optimum impedance matching and good CP radiation.

To reduce electromagnetic interferences (EMI), the most common method is to add a filter (low pass or band pass type) between the antenna and the active radio-frequency (RF) circuit. However, such design will incur additional insertion losses and further complicates the

Correspondence to: W. C. Weng; e-mail: wcweng@ncnu.edu.tw

DOI: 10.1002/mmce.20867

Published online 6 November 2014 in Wiley Online Library (wileyonlinelibrary.com).

RF-circuit design. Therefore, antenna designs with harmonic suppression capability were studied using either the photonic band gap (PBG) method [9, 10], or applying the defected ground structure (DGS) method [11, 12]. By comparing these two methods, the PBG type requires much more complicated periodic structure designs than the DGS type. Notably, other techniques such as introducing a T-shaped [13] or U-shaped [14] parasitic strip into a slot antenna can also achieve harmonic suppression with wide suppressing band. Nevertheless, from the open-literature, there is no reported article on integrating a simple DGS into an ARSA with CP radiation.

Compared with the work in [8], in this study, a compact size 50 × 60 × 0.8 mm^3 microstrip-fed ARSA with CP radiation is proposed for Worldwide Interoperability for Microwave Access (WiMAX) 2.3 GHz (2305–2320/2345–2360 MHz) and Wireless Local Area Network (WLAN) 2.4 GHz (2400–2480 MHz) applications. Instead of applying complicated microstrip feed line and loading an additional vertical slot [8] into the annular-ring slot, in this case, the CP radiation was simply achieved by extending an inverted L-shaped slot from the bottom of the ring slot. Besides exhibiting a wide 10-dB impedance bandwidth measured between 1690 and 2760 MHz, this proposed ARSA has also exhibited broad CP bandwidth of approximately 7.97% (2290–2480 MHz).

To achieve harmonic suppression on a conventional ARSA, the work in [15, 16] have proposed the method of integrating an inverted C-shaped DGS into the bottom section of the annular-ring slot. Notably, this work reported in here is a follow-up of [16], which is not a CP type. By integrating an inverted C-shaped DGS into [16], besides achieving a slightly improve CP bandwidth (9.68%, 2260–2490 MHz), this harmonic suppressed CP ARSA with DGS also act as a low-pass filter, in which all harmonic modes excited above the 3 GHz band are successfully suppressed below the 3-dB half-power threshold. Typical simulations were carried out to demonstrate the accuracy of the two CP ARSA designs (with and without DGS), and the simulated results were compared with actual measurements of the fabricated prototypes.

II. ANTENNAS STRUCTURE

Figure 1 shows the configuration and detailed dimensions of the proposed CP ARSA that is composed mainly of three sections; namely, the annular-ring slot, inverted L-shaped slot, and microstrip-fed line with quarter-wavelength impedance transformer. Here, the proposed antenna with a ground plane size of 50 × 60 mm^2 is fabricated using an inexpensive 0.8 mm thick FR4 substrate with dielectric constant of 4.4 and loss tangent of 0.02. The inner and outer radius of the annular-ring slot are $R_1 = 13.5$ mm and $R_2 = 16$ mm, respectively. The width of the inverted L-shaped slot is $W = 2$ mm, and its total length of 31 mm (20 mm + L) is approximated as one quarter-wavelength of 2.4 GHz, in which the vertical length $L = 11$ mm. The main reason for designing such length of 31 mm is because it will aid in exciting a CP resonant mode at approximately 2.4 GHz. Notably, this inverted L-shaped slot can also be restructured as a horizontal slot of length 31 mm, however, the wide of the antenna (50 mm) will have to be increased in order to accommodate this length. Lastly, the microstrip-fed line is comprised of two rectangular strips connected by a quarter-wavelength impedance transformer. The dimensions of the upper and lower strip line are 3 × 11.25 mm^2 and 2 × 5 mm^2, respectively, while the size of the impedance transformer is 0.7 × 11.5 mm^2.

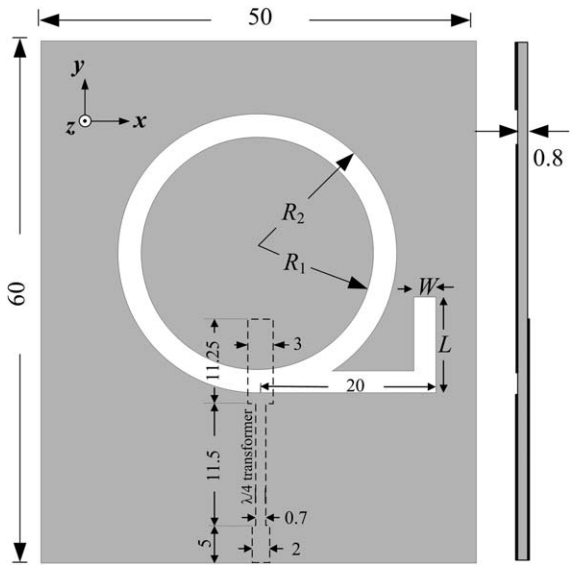

Figure 1 Geometry of proposed CP ARSA, $R_1 = 13.5$, $R_2 = 16$, $L = 11$, $W = 2$. Unit: mm.

Figure 2 shows the geometry of the harmonic suppressed CP ARSA with DGS. The DGS can be perceived

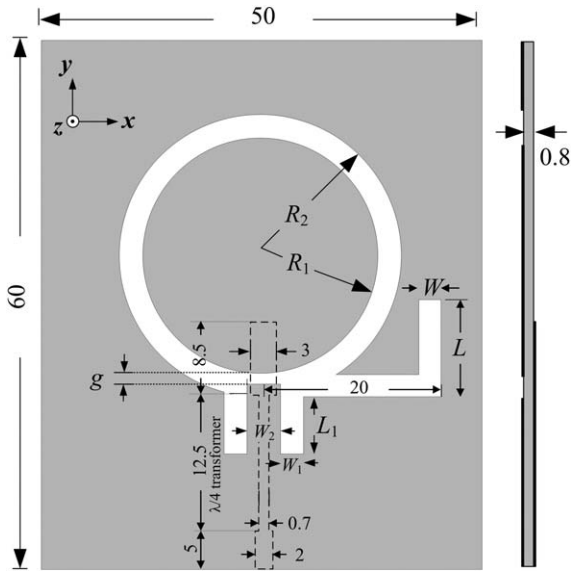

Figure 2 Geometry of proposed harmonic suppressed CP ARSA (with DGS), $R_1 = 12.75$, $R_2 = 15.75$, $L = 12$, $g = 0.75$, $L_1 = 6.5$, $W = 2$, $W_1 = 2.5$, $W_2 = 4$. Unit: mm.

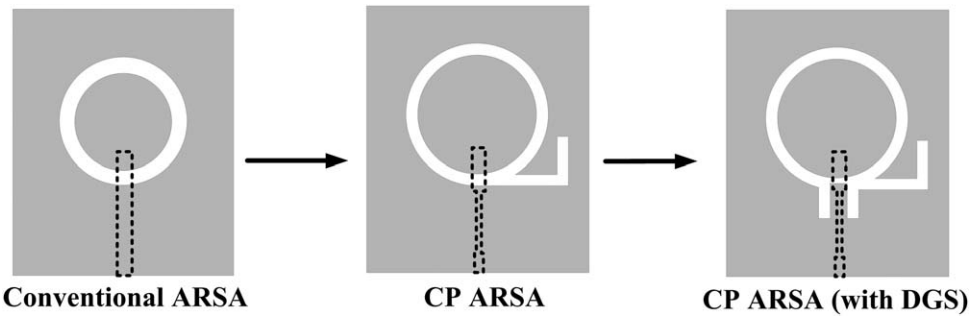

Figure 3 Design evolution of the two proposed CP ARSA.

as an inverted C-shaped slot or as a pair of vertical slot structure loaded at the bottom of the annular-ring slot. The two vertical slots have a same size of $W_1 \times L_1$ (2.5 $\times$ 6.5 mm^2), and they are 4 mm (W_2) apart from each other. Because of this loaded DGS, the gap distant between the inner radius and the bottom ground is devised to be $g = 0.75$ mm, and the dimensions of other vital parameters such as the annular-ring slot ($R_1 = 12.75$ mm, $R_2 = 15.75$ mm), length of inverted L-shaped slot ($L = 12$ mm) and microstrip-fed line must also be slightly altered, so that this proposed CP ARSA with DGS can excite good CP radiation at approximately 2.4 GHz band, while harmonic suppression (stop band) between 3 and 10 GHz can also be attained.

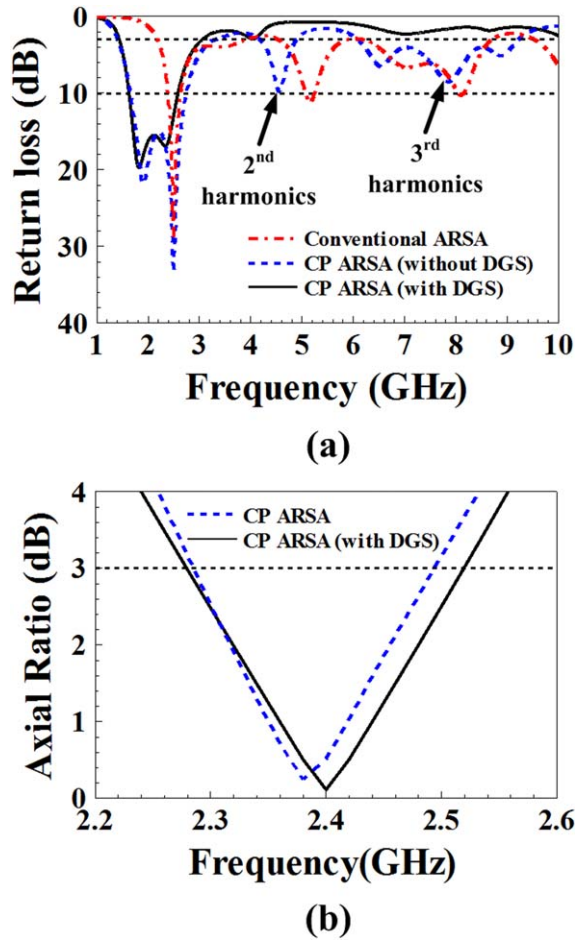

Figure 4 Simulated results of conventional ARSA, CP ARSA, and CP ARSA with DGS, (a) return loss, (b) AR.

III. DESIGN EVOLUTION

The design evolution of the two proposed CP ARSAs can be observed in Figure 3. In this figure, a conventional ARSA was initial studied and designed by using the commercial electromagnetic software HFSS (high frequency structure simulator). To excite good fundamental TM_{11} mode at 2.4 GHz, its inner and outer ring slot radius was devised as 10 mm and 13.5 mm, respectively. From the simulated return loss diagram shown in Figure 4a, besides exhibiting a fundamental mode at 2.4 GHz with 10-dB impedance bandwidth of 2.38–2.63 GHz, three distinctive harmonic modes at approximately 5, 7 and 8 GHz were also observed from this conventional ARSA.

By loading the inverted L-shaped slot into the conventional ARSA, follow by altering the dimension of some of the vital parameters (see Fig. 1), besides the ability to excite CP radiation, this proposed CP ARSA has also demonstrated broad 10-dB impedance bandwidth of 1.65–2.74 GHz. Notably, the excitation of this CP radiation is due to the total length of the inverted L-shaped slot that is approximately 1/4 wavelength long (31 mm) at 2.4 GHz, and is extended directly from the bottom of the ring slot. By doing so, two orthogonal modes with equal amplitudes can then be generated.

As shown in Figure 4, two distinct harmonic modes (2nd and 3rd harmonics) at 4.8 and 7.85 GHz were observed, respectively. To suppress the harmonic modes (below 3-dB threshold), as shown in Figure 4a, the DGS was introduced into the CP ARSA (see Fig. 3), and by further observing Figure 4a, although the 10-dB impedance bandwidth was reduced to 1.62–2.58 GHz, however, all the harmonic modes exhibited in the CP ARSA were successfully suppressed. Figure 4b shows the simulated AR diagrams of the two CP ARSA (with and without DGS). In this figure, the 3-dB AR bandwidth of the proposed CP ARSA with DGS (2.28–2.52 GHz) was slightly larger than its counterpart without the DGS (2.27–

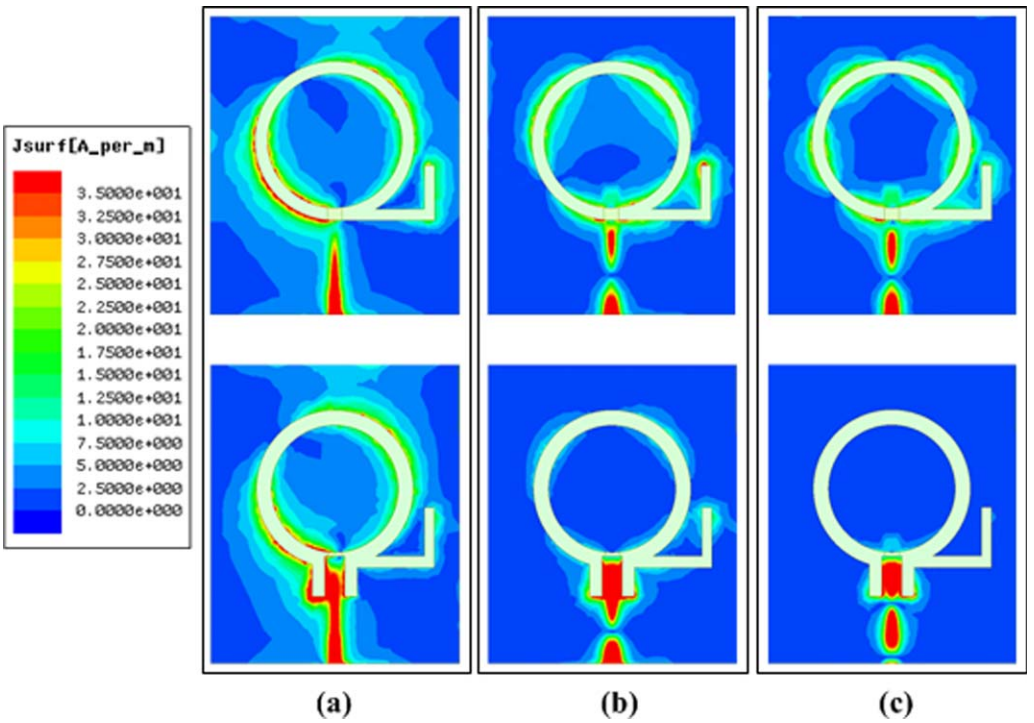

Figure 5 Simulated current distribution diagrams of the two proposed CP ARSAs (with and without DGS), (a) 2.4 GHz, (b) 4.8 GHz, and (c) 7.85 GHz.

2.49 GHz). Furthermore, it has also demonstrated better CP performance of AR = 0.114 dB at 2.4 GHz.

To further comprehend how the introduction of the DGS can aid in suppressing the higher order harmonic modes, the current distribution diagrams of the two proposed CP ARSA (with and without DGS) were plotted and compared in Figure 5. For brevity, only three frequencies were selected, namely, the fundamental frequency (2.4 GHz), 2nd harmonic frequency (4.8 GHz) and 3rd harmonic frequency (7.85 GHz). Figure 5a shows that at 2.4 GHz, the two proposed antennas have demonstrated similar current distributions along the annular-ring slot. However, as depicted in Figures 5b and (c), the current distributions of the two higher order harmonic frequencies were confined by the DGS, and very little currents were allowed to flow along the annular-ring slot.

IV. PARAMETRIC STUDIES

The simulation of the two proposed CP ARSA were conducted using the software HFSS. By applying this software, the initial performances of the proposed antenna can be obtained without performing any hands on experiment. Furthermore, the vital parameters of the antenna that can affect the impedance bandwidth and CP performance can also be attained and evaluated.

Via the simulation, the following three parameters, namely, R_2, L, and W, have exhibited distinct changes in the antenna performances. Therefore, for brevity, this paper shows the parametric studies of these three parameters for CP ARSA only.

The effects of tuning the outer radius R_2 of annular-ring slot are shown in Figure 6. As shown in Figure 6a, a step increment in R_2 by 0.5 mm (from 13 to 14 mm) will result in slightly shifting the upper resonant frequency from 2.51 to 2.49 GHz, whereas slight changes were also observed at the lower resonant frequency. Here, because of the shifting in the upper resonant frequency to the lower frequency band, besides a slightly reduced 10-dB impedance bandwidth, a linearly decreased AR frequency (from 2.48 to 2.34 GHz) was also observed with corresponding to the step increased in parameter R_2, as shown in Figure 6b.

The effects of tuning the length L of the inverted L-shaped slot are shown in Figure 7. For a conventional ARSA, a distinct resonant frequency at ~2.5 GHz was observed in Figure 7a, and because it was a linearly polarized type (with large AR values), thus, it is not included in Figure 7b. For the case when $L = 0$ mm, an AR value of ~6 was observed at 2.58 GHz. However, if L was further increased from 5.5 to 13 mm, it can be observed in Figure 7a that an additional resonant frequency at the lower frequency band (below 2 GHz) will be excited, which is responsible for exciting good CP radiation as shown in Figure 7b. For the case when $L = 11$ mm, good AR value of 0.26 was achieved at 2.38 GHz.

The effects of tuning the slot width W of the inverted L-shaped slot are shown in Figure 8. As depicted in Figure 8b, a slight decrement in W by 1 mm (from 3 to 1 mm) will lead to a linear variation of the CP frequency, in which a linear shift from ~2.48 to 2.25 GHz was observed. When $W = 1$ mm, an impedance mismatch was

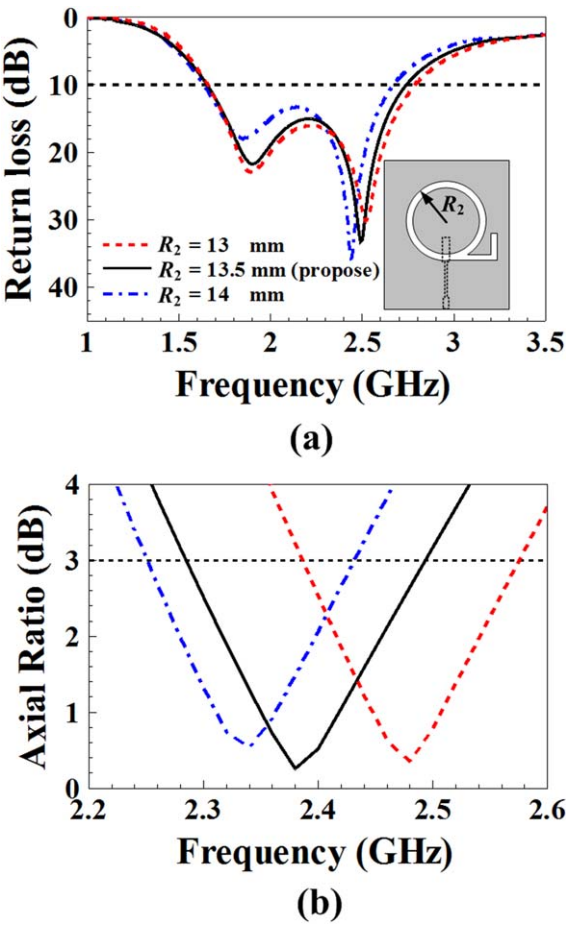

Figure 6 Proposed CP ARSA (without DGS) with different lengths R_2, (a) return loss, (b) AR.

observed in Figure 8a between the two resonant frequencies. In contrast, tuning W between 1 and 2 mm has minor effects on the two resonant frequencies, and good CP performance can be attained at 2.38 and 2.48 GHz. Here, $W = 2$ mm was chosen because the 3-dB AR bandwidth can cover both WiMAX 2.3 GHz and WLAN 2.4 GHz bands.

Figure 9 shows the effects of tuning the DGS length L_1 of the harmonic suppressed CP ARSA. As depicted in Figure 9a, a linear step decrement in L_1 by 1 mm (from 7.5 to 5.5 mm) has minor effects on the two resonant frequencies, however, at $L_1 = 5.5$ mm, the harmonic mode at ~4.2 GHz was larger than the 3-dB half-power threshold limit. As shown in Figure 9b, although broad 3-dB AR bandwidth between 2.2 and 2.51 GHz was observed when $L_1 = 7.5$ mm, however, an AR value of 1.36 was observed at 2.36 GHz. Thus, in this case, $L_1 = 6.5$ mm was chosen, because it can excite an AR value of 0.11 at exactly 2.4 GHz with 3-dB AR bandwidth of between 2.28 and 2.52 GHz.

Lastly, the effects of tuning the DGS slot width W_1 of the harmonic suppressed CP ARSA are shown in Figure 10. As depicted in Figure 10b, a slight increment in W_1 by 1 mm (from 3 to 5 mm) will lead to a linear variation of the CP frequency, in which a linear shift from ~2.35 to 2.44 GHz was observed. Notably, as shown in Figure 10a, at $W_1 = 3$ mm, the two resonant frequencies are integrated with each other, and the harmonic mode at approximately 4.2 GHz was also larger than the 3-dB half-power threshold limit. When $W_1 = 5$ mm, although a good AR value of 0.23 was also observed at 2.44 GHz, its 3-dB AR bandwidth (2.31–2.55 GHz) cannot satisfy the WiMAX 2.3 GHz band. Therefore, in this case, $W_1 = 4$ mm was chosen for the proposed design.

Based on the aforementioned parametric studies, the following design guidelines can be concluded; (1) The loading of an inverted L-shaped slot into a conventional ARSA was responsible for exciting an additional resonant frequency at the lower band (< 2 GHz), and follow by tuning the slot length L, good CP radiation can then be achieved. (2) For the CP ARSA, the AR frequency can be linearly varied by tuning radius R_2 and width W. (3) For the CP ARSA with a DGS, the AR frequency can also be linearly varied by tuning the length L_1 and width W_1 of the DGS. However, the harmonic mode located at ~4.2 GHz must be carefully observed as it may exceed the 3-dB half-power threshold.

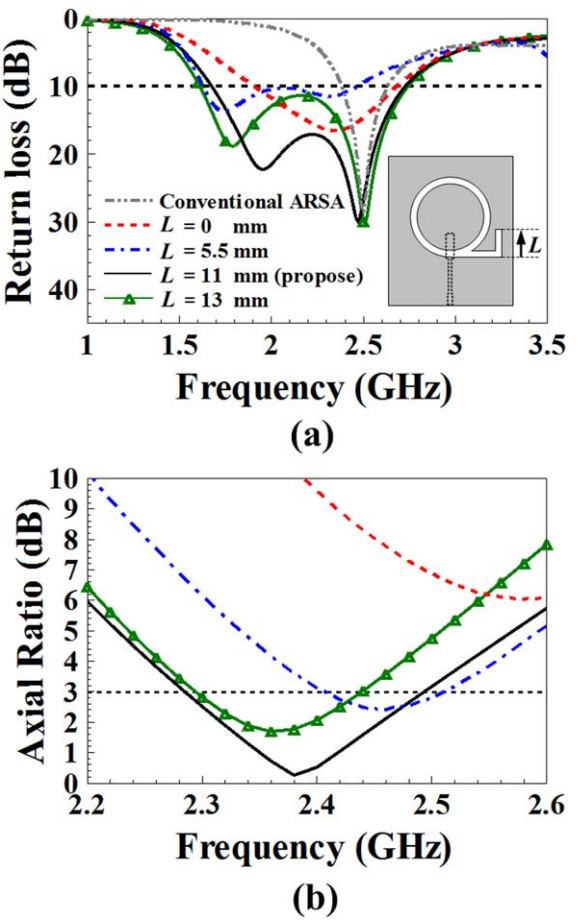

Figure 7 Proposed CP ARSA with different inverted L-shaped slot lengths L, (a) return loss, (b) AR.

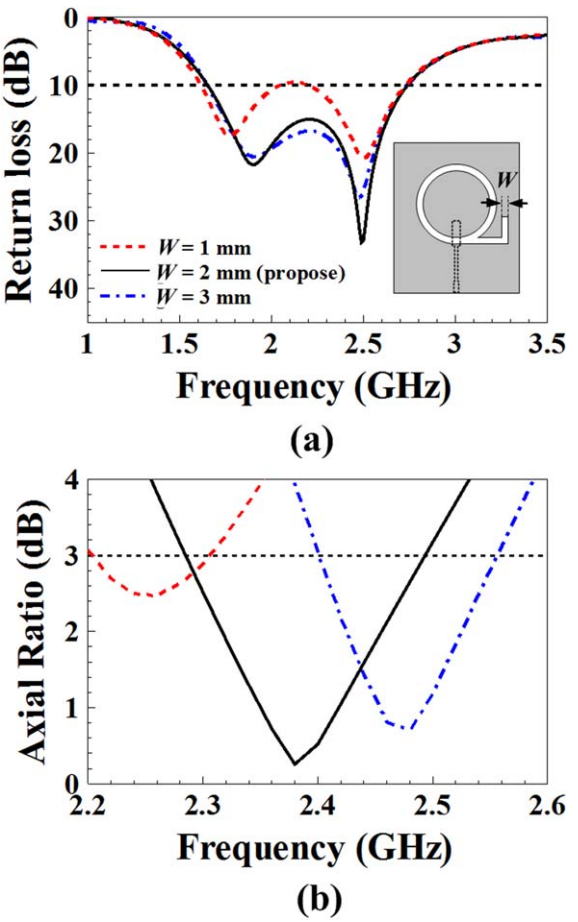

Figure 8 Proposed CP ARSA with different widths (W) of the inverted L-shaped slot, (a) return loss, (b) AR.

V. RESULTS AND DISCUSSION

The simulated and measured return loss and axial ratio (AR) of both proposed CP ASRAs (with and without DGS) for WiMAX 2.3 GHz and WLAN 2.4 GHz applications are shown in Figures 11a and 11b, respectively. The measured results were consistent with the simulated ones. As depicted in Figure 11a, the measured 10-dB impedance bandwidths of CP ARSA and CP ASRA with DGS were 48.09% (1690–2700 MHz) and 44.86% (1660–2620 MHz), respectively. Furthermore, from the measured results, the CP ARSA with DGS can successfully suppress all the harmonic modes at above 3 GHz. Figure 11b shows the simulated and measured 3-dB AR bandwidth of the two CP ARSAs. In this figure, a good agreement was observed between the simulated and measured results, and the slight discrepancy between them may be because of the soldering effects and dielectric loss of the FR4 substrate. Here, the measured 3-dB AR bandwidth of the CP ARSA was 190 MHz (7.97%, 2290–2480 MHz). In comparison, the harmonic suppressed CP ARSA with DGS has exhibited wider 3-dB AR bandwidth of 250 MHz (9.68%, 2260–2490 MHz). This phenomenon was also validated by the simulation.

The measurements (including radiation patterns, peak gain, and radiation efficiency) of the two proposed CP ARSAs were conducted in a far-field anechoic chamber (NSI 800F-10/*WavePro* FFC-. 700S) for 0.8–18 GHz antenna tests. Figure 12 shows the measured and simulated far-field radiation patterns (normalized) of the proposed CP ASRA with DGS in the two principal planes (x-z and y-z planes) at 2400 MHz. Because the measured radiation patterns for the CP ARSA (without DSG) have also exhibited very similar patterns, thus, for brevity, it was not shown in this article. At boresight (+z) direction, good broadside pattern was plotted for the left-hand CP (LHCP), while the (–z) direction has presented similar broadside pattern for the right-hand CP (RHCP).

Figure 13 shows the measured boresight peak gain level and radiation efficiency of the two proposed CP ARSAs between 2.3 and 2.5 GHz. In this figure, the CP ARSA has demonstrated stable gain level (5.06–5.41 dBic) and radiation efficiency (76–81%). In comparison, the harmonic suppressed CP ARSA with DGS has exhibited slightly lower gain level (4.55–4.82 dBic) and radiation efficiency (70–73%). The harmonic suppressed CP ARSA with DGS has lower gain and efficiency level of

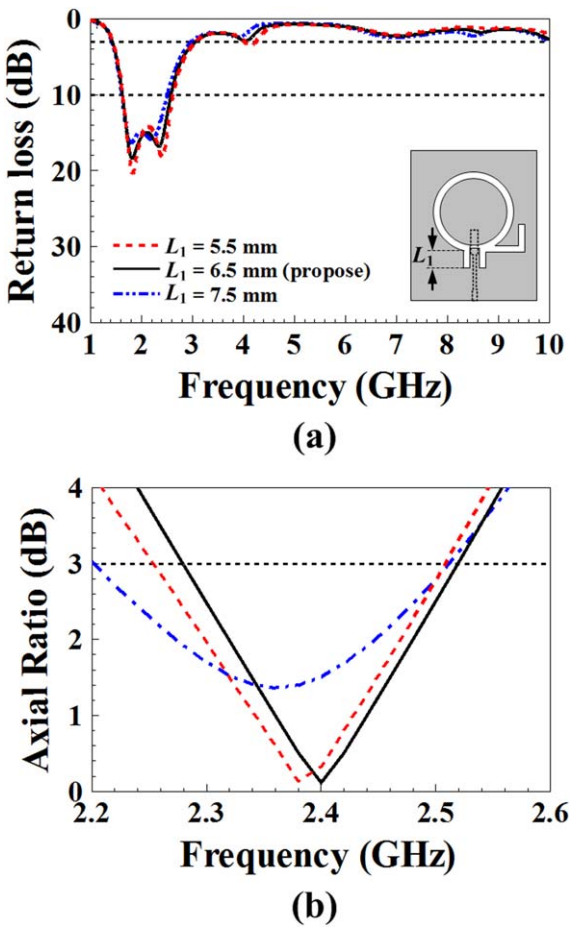

Figure 9 Proposed harmonic suppressed CP ARSA (with DGS) with different DGS lengths L_1, (a) return loss, (b) AR.

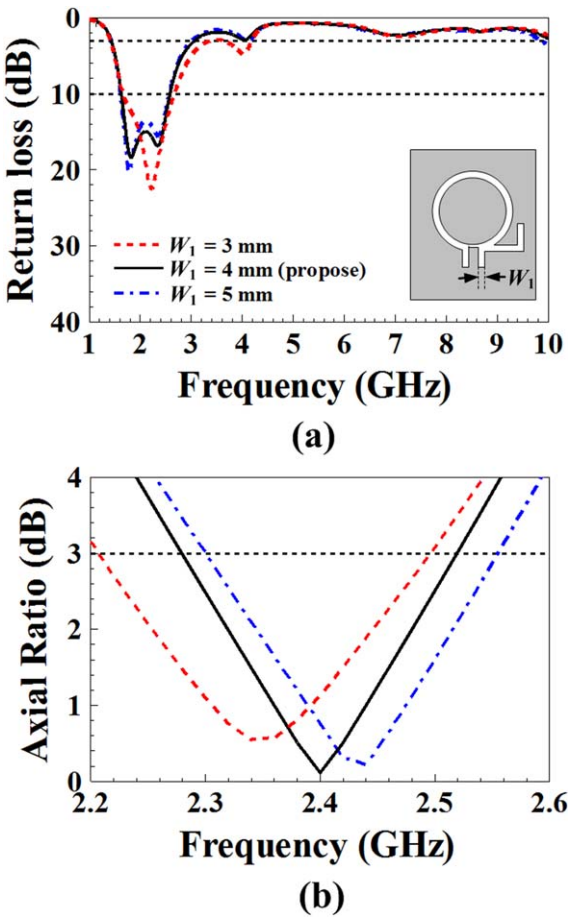

Figure 10 Proposed harmonic suppressed CP ARSA (with DGS) with different DGS width W_1, (a) return loss, (b) AR.

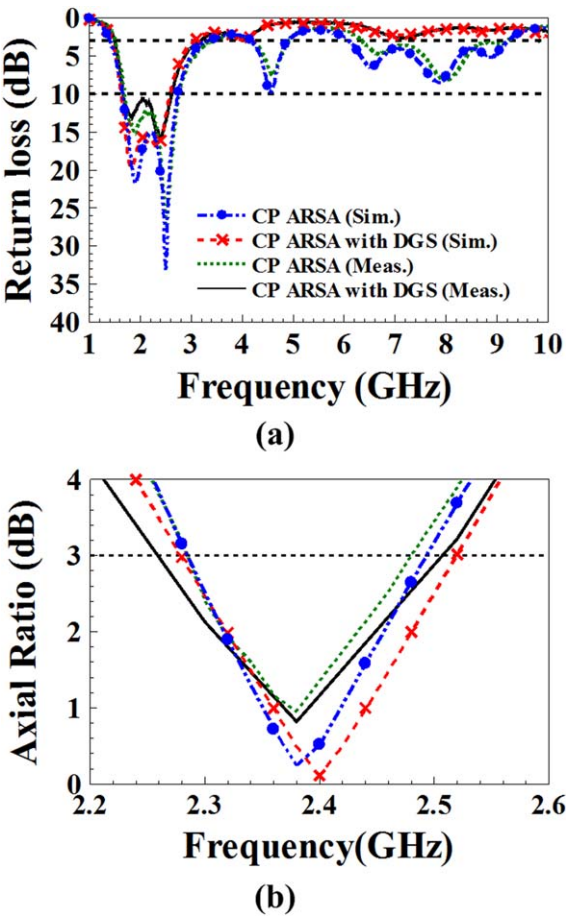

Figure 11 Simulated and measured results of the two proposed CP ARSAs, (a) return losses, (b) AR.

$\sim$0.5 dB and 7% in average, respectively, than that of the CP ARSA. This level of drop in gain and efficiency results coincide with the results reported in [17], in which a DGS was also integrated into a CP slot antenna, and a slight reduction in gain and efficiency were also observed. Therefore, it can be concluded that although the devised DGS can improve the CP bandwidth of the proposed CP ARSA and successfully suppressed the harmonic modes at >3 GHz, the downside of this DGS design was a slightly degraded gain and efficiency.

Table I shows the measured peak gains of CP ARSA (with and without loading the DGS) at fundamental mode and two harmonic modes. As shown in this table, a small reduction in peak gain (circular polarization, CP) of 0.49 dB at fundamental mode (2.4 GHz) was observed. In contrast, due to the harmonic suppression of the second and third harmonics, reduction in peak gain (linear polarization) of $\sim$10 dB were observed at these two harmonics.

Table II shows the comparison between the proposed CP ARSA and various slot antennas with different DGS methods for harmonic suppression purpose. For the case of [11] that employed the method of H-shaped DGS, narrow stop band was observed because of undesirable dips at 4.5 and >6 GHz bands. As for the case in [12], although it has demonstrated a wide stop band between 3.2 and 12 GHz, two partial rings were required to be

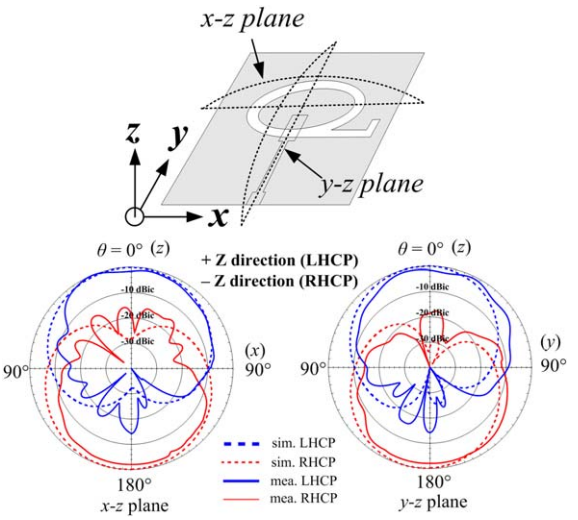

Figure 12 Simulated and measured radiation patterns of the harmonic suppressed CP ARSA with DGS in the two principal planes, *x-z* plane and *y-z* plane.

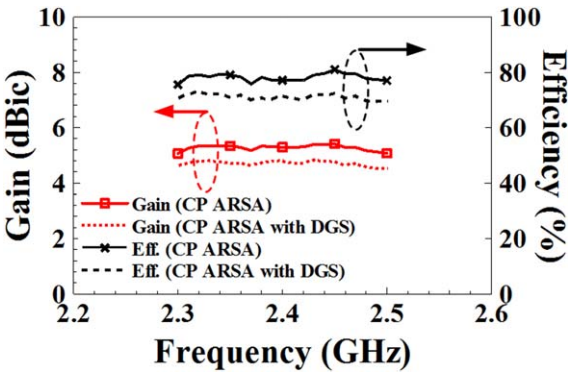

Figure 13 Measured peak gain and efficiency variation of the two proposed CP ARSAs.

TABLE I Measured Peak Gain Comparison of CP ARSA (With and Without Loading the DGS) in Various Modes

Mode (Frequency)	Measured Gain (without DGS)	Measured Gain (with DGS)
Fundamental (2.4 GHz)	5.29 dBic	4.8 dBic
Second Harmonic (4.8 GHz)	5.02 dBi	−5.18 dBi
Third Harmonic (8.1 GHz)	6.15 dBi	−4.02 dBi

loaded side by side along the microstrip-fed line, which results in requiring a long feeding line. Lastly, the case in [16] was similar to the proposed one, however, its fundamental mode cannot excite CP radiation (so does [11] and [12]), furthermore, the stop band of [16] was between 3 and 8.6 GHz. In comparison, besides the ability to excite CP radiation at the fundamental mode, the proposed one has also exhibited wider stop band of between 3 and 10 GHz.

VI. CONCLUSIONS

In this design, a simple method of loading an inverted L-shaped narrow slot into a microstrip-fed ARSA was initially introduced to excite good CP radiations at 2.4 GHz. This proposed CP ARSA has exhibited 10-dB impedance bandwidth and CP bandwidth of ∼48 and 8%, respectively. Here, an average gain and efficiency of ∼5.2 dBic and 78% were also measured, respectively. To further achieve harmonic suppression over frequencies larger than 3GHz for this proposed CP antenna, the technique of loading an inverted C-shaped DGS into the proposed CP ARSA was proposed. By this way, the proposed CP ARSA with DGS has demonstrated wider CP bandwidth of 9.68%, and an average gain and efficiency level of ∼4.7 dBic and 71% were also presented. Because the CP bandwidth of the two proposed CP ARSAs can cover operating frequencies between 2.3 and 2.48 GHz, therefore, they can be applied for both WiMAX 2.3 GHz and WLAN 2.4 GHz applications.

TABLE II Comparison Between the Proposed Antenna and Reference Antennas With DGS for Harmonic Suppression

Ant.	Size (mm^3)	Stop Band (GHz)	DSG Method
[11]	52 × 52 × 0.5[a]	1.81–4.40	H-shaped DGS
[12]	UI × UI × 0.5[a]	3.20–12.0	Partial-ring DGS
[16]	50 × 60 × 0.8	3.00–8.60	Inverted-C DGS
proposed	50 × 60 × 0.8	3.00–10.0	Inverted-C DGS

[a]Roger Substrate.
UI: Unidentified.

REFERENCES

1. P.C. Sharma and K.C. Gupta, Analysis and optimized design of single feed circularly polarized microstrip antennas, IEEE Trans Antennas Propag 31 (1983), 949–955.
2. Nasimuddin, X. Qing , and Z.N. Chen, Dual-square-ring-shaped slot antenna for wideband circularly polarized radiation, Microwave Opt Technol Lett 56 (2014), 2645–2649.
3. C.J. Wang and C.H. Chen, CPW-fed stair-shaped slot antennas with circular polarization, IEEE Trans Antennas Propag 57 (2009), 2483–2486.
4. J.Y. Sze, C.I.G. Hsu, Z.W. Chen, and C.C. Chang, Broadband CPW-fed circularly polarized square slot antenna with lightening-shaped feed-line and inverted-L grounded strips, IEEE Trans Antennas Propag 58 (2010), 973–977.
5. Nasimuddin, Z. N. Chen, and X. Qing, Symmetric-aperture antenna for broadband circular polarization, IEEE Trans Antennas Propag 59 (2011), 3932–3936.
6. K.L. Wong, C.C. Huang, and W.S. Chen, Printed ring slot antenna for circularly polarization, IEEE Trans Antennas Propag 50 (2002), 75–772.
7. W.S. Chen, C.C. Huang, and K.L. Wong, Microstrip-line-fed printed shorted ring-slot antennas for circular polarization, Microwave Opt Technol Lett 31 (2001), 137–140.
8. J.Y. Sze, C.I.G. Hsu, M.H. Ho, Y.H. Ou, and M.T. Wu, Design of circularly polarized annular-ring slot antenna fed by a double-bent microstrip line, IEEE Trans Antennas Propag 55 (2007), 3134–3139.
9. Y. Horii and M. Tsutsumi, Harmonic control by photonic bandgap on microstrip patch antenna, IEEE Microwave Guid Wave Lett, 9 (1999), 13–48.
10. X.C. Lin and L.T. Wang, A broadband CPW-Fed loop slot antenna with harmonic control, IEEE Antennas Wireless Propag Lett 2 (2003), 323–325.
11. Y.J. Sung, M. Kim, and Y.S. Kim, Harmonics reduction with defected ground structure for a microstrip patch antenna, IEEE Trans Antennas Wireless Propag Lett 2 (2003), 111–113.
12. S. Biswas, G. Debatosh, and K. Chandrakanta, Control of higher harmonics and their radiations in microstrip antennas using compact defected ground structures, IEEE Trans Antennas Propag 61 (2013), 3349–3353.
13. N.A. Nguyen, R. Ahmad, Y.T. Im, Y.S. Shin, and S.O. Park, A T-shaped wide-slot harmonic suppression antenna, IEEE Antennas Wireless Propag Lett 6 (2007), 647–650.
14. D.H. Choi, Y.J. Cho, and S.O. Park, A broadband slot antenna with harmonic suppression, Microwave Opt Technol Lett 48 (2006), 1984–1987.
15. J.S. Park, J.H. Kim, J.H. Lee, S.H. Kim, and S.H. Myung, A novel equivalent circuit modeling method for defected ground structure and its application to optimization of a DGS lowpass filter, IEEE Int Microwave Symp Digest 1 (2002), 417–420.

16. C.Y.D. Sim, M.H. Chang, and B.Y. Chen, Microstrip-fed ring slot antenna design with wideband harmonic suppression, IEEE Trans Antennas Propag 62 (2014), 4828–4832.

17. Y. Xu, S. Gong, and T. Hong, Circularly polarized slot microstrip antenna for harmonics suppression, IEEE Trans Antennas Wireless Propag Lett 12 (2013), 472–475.

BIOGRAPHIES

Chow-Yen-Desmond Sim was born in Singapore, on February 26, 1971. He received his BSc degree from the Engineering Department at University of Leicester, UK, in 1998. In 1999, he earned a fee waiver Ph.D scholarship from the Radio System Group, Engineering Department, at University of Leicester, and graduated in July, 2003. In July 2007, he joined the Department of Electrical Engineering, Feng Chia University, Taichung, Taiwan as an associate professor, where he became a full professor in 2012. He is the author or coauthor of over 70 SCI articles. His current research interests include antenna design, VHF/UHF tropospheric propagation and RFID applications. He is a Fellow of the Institute of Engineering and Technology (FIET), senior member of the IEEE Antennas and Propagation Society, and life-member of the IAET. In July 2014, he was awarded as one of the top 10 reviewers (2013/2014) for IEEE Transactions on Antennas and Propagation. E-mail: cysim@fcu.edu.tw

Wei-Chung Weng received the B.S. degree in electronic engineering from National Changhua University of Education, Changhua, Taiwan, in 1993, the M.S. degree in electrical engineering from I-Shou University, Kaohsiung, Taiwan, in 2001, and the Ph.D. degree in electrical engineering from The University of Mississippi, USA, in 2007. In 2008, he joined the Department of Electrical Engineering, National Chi Nan University, Puli, Taiwan, as an Assistant Professor. He has been an Associate Professor at the same university since 2014. His research interests include antennas and microwave circuits design, numerical methods in electromagnetics, electromagnetic compatibility, and optimization techniques in electromagnetics. He has served many journals as a Reviewer. He is the coauthor of the book entitled Electromagnetics and Antenna Optimization Using Taguchi's Method (Morgan & Claypool, 2008). Dr. Weng is a Senior Member of the IEEE Antennas and Propagation Society, a member of the Applied Computational Electromagnetic Society (ACES), and a Life-member of the Institute of Antenna Engineers of Taiwan (IAET). E-mail: wcweng@ncnu.edu.tw

Ming-Hsuan Chang was born in Taichung, Taiwan, R.O.C., on July 5, 1988. In June, 2010, he received his Bachelor degree from the Department of Communication Engineering at Feng Chia University, Taiwan, R.O.C. In June, 2013, he received his Master Degree from the Department of Electrical Engineering at the same university. He was an active research member of the Antenna and Propagation Laboratory in the Department of Electrical Engineering, Feng Chia University, between 2011 and 2013. He is now working as a research engineer in TDK Taiwan Corporation. His current research interests include antenna design, RF circuit design, and wireless energy transfer. E-mail: m9949556@fcu.edu.tw

Bo-Yu Chen was born in Yilan, Taiwan, R.O.C., on December 21, 1990. In June, 2013, he received his Bachelor degree from the Department of Electrical Engineering at Feng Chia University, Taiwan, R.O.C. He is now working towards his Master Degree in the same department. He is an active research member of the Antenna and Propagation Laboratory in the Department of Electrical Engineering, Feng Chia University, since 2011. His current research interests are in RFID, array and CP antenna design. E-mail: m0203723@fcu.edu.tw